S-Ribosylhomocysteinase (LuxS) Is a Mononuclear Iron Protein†

Jinge Zhu, Eric Dizin, Xubo Hu, Anne-Sophie Wavreille, Junguk Park, and Dehua Pei*

Department of Chemistry and Ohio State Biochemistry Program, The Ohio State University, 100 West 18th Avenue, Columbus, Ohio 43210

Received February 20, 2003; Revised Manuscript Received March 10, 2003

ABSTRACT: *S*-Ribosylhomocysteinase (LuxS) catalyzes the cleavage of the thioether linkage of *S*-ribosylhomocysteine (SRH) to produce L-homocysteine and 4,5-dihydroxy-2,3-pentanedione (DHPD). This is a key step in the biosynthetic pathway of the type II autoinducer (AI-2) in both Gram-positive and Gram-negative bacteria. Previous studies demonstrated that LuxS contains a divalent metal cofactor, which has been proposed to be a Zn^{2+} ion. To gain insight into the catalytic mechanism of this unusual reaction and the function of the metal cofactor, we developed an efficient expression and purification system to produce LuxS enriched in either Fe^{2+}, Co^{2+}, or Zn^{2+}. Comparison of the catalytic properties and stability of the metal-substituted LuxS with those of the native enzyme revealed that the native metal ion is Fe^{2+}. The electronic absorption spectrum of the Co(II)-substituted LuxS underwent dramatic catalysis-dependent changes, suggesting the direct involvement of the metal ion in catalysis. Site-directed mutagenesis studies showed that Glu-57 and Cys-84 are essential for catalysis, most likely acting as general acids/bases. Reaction in D_2O resulted in the incorporation of deuterium at the C-1, C-2, and C-5 positions of the diketone product. These data suggest a catalytic mechanism in which the metal ion catalyzes an intramolecular redox reaction, shifting the carbonyl group from the C-1 position to the C-3 position of the ribose. Subsequent β-elimination at the C-4 and C-5 positions releases homocysteine as a free thiol.

Quorum sensing is the mechanism by which many bacteria control gene expression in response to cell density. This cell−cell communication is mediated by the synthesis and detection of small molecules called autoinducers (AIs)[1] (reviewed in ref *1*). Gram-negative bacteria generally employ acylated homoserine lactones as AIs, whereas Gram-positive bacteria tend to use peptide derivatives. Recently, a second quorum-sensing system (AI-2), which is shared by both Gram-negative and positive bacteria, has been discovered (*2*). Unlike AI-1s, which have species-specific structures, AI-2 is a universal signal utilized by all bacteria, presumably for interspecies communication. AI-2 is the adduct of borate and a ribose derivative and is produced from *S*-adenosylhomocysteine (SAH) (*3*). SAH is the byproduct of numerous transmethylation reactions involving *S*-adenosylmethionine (SAM). Hydrolysis of SAH by the nucleosidase Pfs yields *S*-ribosylhomocysteine (SRH) and adenine (Figure 1). SRH is then converted to homocysteine and 4,5-dihydroxy-2,3-pentanedione (DHPD) by *S*-ribosylhomocysteinase (LuxS) (*4*−*6*). DHPD spontaneously cyclizes to form a furanone, which is complexed with borate to form AI-2 (*3*).

The reaction catalyzed by LuxS is mechanistically unprecedented. It is formally the nonredox cleavage of a stable thioether bond. Eukaryotic cells contain a similar activity in SAH hydrolase, which utilizes NAD^+ to oxidize the 3′-OH group into a ketone intermediate (*7*). Subsequent β-elimination at the C4′ and C5′ positions cleaves the thioether bond to release a homocysteine. However, LuxS does not require NAD^+ or any other redox-active cofactors for activity. Through structural genomic efforts, several X-ray crystal structures of LuxS, both in its free form and with bound substrate/product, have been reported (*8*−*10*). LuxS exists as a homodimer, and two identical active sites are formed at the dimer interface. Each active site contains a divalent

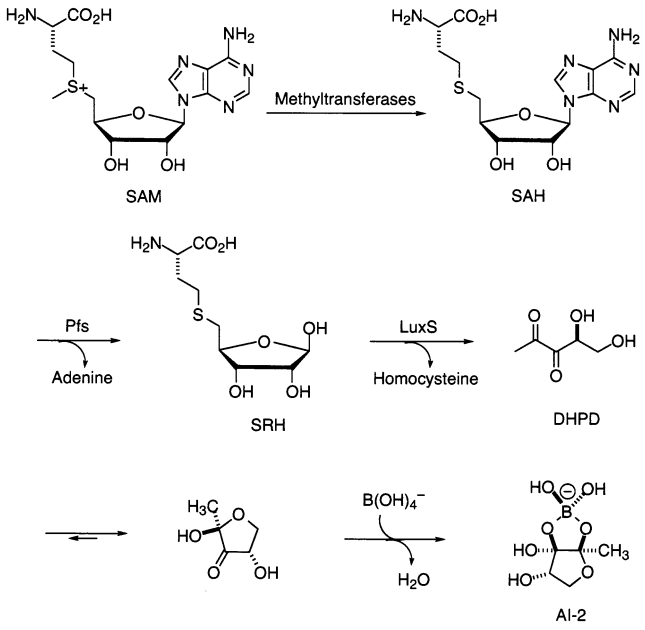

FIGURE 1: Biosynthetic pathway of AI-2.

† This work was supported by grants from the National Institutes of Health (AI40575 and GM62820 to D.P.).

* To whom correspondence should be addressed. Telephone: (614) 688-4068. Fax: (614) 292-1532. E-mail: pei.3@osu.edu.

[1] Abbreviations: SAH, *S*-adenosylhomocysteine; SAM, *S*-adenosylmethionine; SRH, *S*-ribosylhomocysteine; DHPD, 4,5-dihydroxy-2,3-pentanedione; AI, autoinducer; PCR, polymerase chain reaction; DTNB, 5,5′-dithiobis(2-nitrobenzoic acid); ESI-MS, electrospray ionization mass spectrometry.

10.1021/bi034289j CCC: $25.00
Published on Web 04/03/2003

metal ion, which has been proposed to be a Zn^{2+} ion (*8*−*10*). The metal ion is tetrahedrally coordinated by a water molecule and three conserved residues (His-54, His-58, and Cys-126 in *Bacillus subtilis* LuxS). Such a ligand environment suggests a catalytic role for the metal ion, but there has been no mechanistic study on LuxS, and it is unclear how the metal ion might participate in catalysis. Other investigators have previously made some puzzling observations, such as the rapid inactivation of LuxS during purification (*4*, *11*) and the oxidation of an active site cysteine (Cys-84 in *B. subtilis* LuxS) into cysteic acid in the crystal structures (*9*, *10*). To gain mechanistic insight into this unusual enzyme, we have overexpressed the *B. subtilis* LuxS in *Eschericia coli* and purified the recombinant enzyme to near homogeneity. Our studies show that LuxS is a novel Fe^{2+} enzyme, and oxidation of the Fe^{2+} cofactor is responsible for the observed instability and cysteine-84 oxidation. A catalytic mechanism involving the metal ion as a key Lewis acid has been proposed.

MATERIALS AND METHODS

Materials. SAH and 1,2-phenylenediamine were purchased from Sigma-Aldrich. Oligonucleotides were purchased from Integrated DNA Technologies (Coralville, IA). Talon resin was from Clontech Laboratories (Palo Alto, CA). Restriction endonucleases were from New England Biolabs (Beverly, MA). All other chemicals and reagents were purchased from Sigma-Aldrich.

Cloning of LuxS and Site-Directed Mutagenesis. The gene coding for *B. subtilis* LuxS protein (*12*) was cloned by using the polymerase chain reaction (PCR) with genomic DNA as template and primers 5′-GGAAGGCCATATGCCTTCAGTAGAAAGTTTTGAG-3′ and 5′-GAATTCTCGAGTTAGCCAAATACTTTTAGCAATTC-3′. The PCR product was digested with restriction endonucleases *Nde*I and *Xho*I and subcloned into the prokaryotic expression vector pET22b-(+) (Novagen, WI) to generate the plasmid pET22b-luxS. To facilitate its purification, a C-terminally histidine-tagged LuxS variant was also constructed by using 5′-GAATTCTCGAGGCCAAATACTTTTAGCAATTC-3′ as the 3′ PCR primer. The amplified DNA was digested with *Nde*I and *Xho*I and subcloned into pET22b(+) to produce the plasmid pET22b-luxS-HT. Site-directed mutagenesis was carried out on the plasmid pET22b-luxS-HT using the QuikChange mutagenesis kit (Stratagene, CA). The primers used for mutagenesis were as follows: C84A, 5′-GATATTTCTCCAATGGGCGCCCAAACAGGCTATTATC-3′; C84S, 5′-GATATTTCTCCAATGGGCTCCCAAACAGGCTATTATC-3′; C84D, 5′-GATATTTCTCCAATGGGCGACCAAACAGGCTATTATC-3′; E57D, 5′-CATTCACACGCTTGACCATTTGCTCGCGTT-3′; E57Q, 5′-CATTCACACGCTTCAGCATTTGCTCGCGTT-3′; and E57A, 5′-CATTCACACGCTTGCGCATTTGCTCGCGTT-3′. The identity of all DNA constructs was confirmed by DNA sequencing. The wild-type luxS gene contained 14 silent mutations as compared to the previously reported DNA sequence (*12*).

Purification of LuxS and Mutants. *E. coli* BL21(DE3) cells (4 L) carrying the proper plasmid DNA were grown in LB medium supplemented with 75 mg/L ampicillin at 37 °C to an OD_{600} of 0.7. The cells were induced by the addition of 100 μM isopropyl β-D-thiogalactoside and grown at 30 °C for an additional 5 h. Cells were harvested by centrifugation and resuspended in 140 mL of a lysis buffer containing 20 mM Tris·HCl (pH 8.0), 0.5 M NaCl, 5 mM imidazole, 1% Triton X-100, 0.5% protamine sulfate, 20 μg/mL trypsin inhibitor, 50 μg/mL *p*-methylbenzenesulfonyl fluoride, and 70 μg/mL chicken egg white lysozyme. The cells were lysed by stirring for 20 min at 4 °C, followed by brief sonication and centrifugation. For the purification of the histidine-tagged LuxS, the supernatant was loaded on a Talon metal affinity column (Clontech, 3.0 × 2.5 cm) equilibrated in 20 mM Tris·HCl (pH 8.0), 0.5 M NaCl, and 5 mM imidazole. The column was eluted with the above buffer containing 60 mM imidazole. Fractions containing significant amounts of LuxS protein (as analyzed by SDS−PAGE) were pooled and concentrated in an Amicon apparatus (Millipore). Glycerol was added to a final concentration of 33% (v/v), and the enzyme was quickly frozen in liquid nitrogen and stored at −80 °C. For the purification of Co(II)-, Zn(II)-, and Fe(II)-substituted LuxS, cells were grown in minimal media supplemented with 0.25% D-glucose, 2 μg/mL thiamin, 1 μg/mL D-biotin, 0.1% $(NH_4)_2SO_4$, and a metal salt mixture (0.5 mM $MgSO_4$, 0.5 μM H_3BO_3, 0.1 μM $MnCl_2$, 0.5 μM $CaCl_2$, 10 μM $CuSO_4$, 1 nM ammonium molybdate). $CoCl_2$, $ZnSO_4$, and $Fe(NH_4)_2(SO_4)_2$ were added to the media at the time of induction to a final concentration of 100 μM, respectively. The non-histidine-tagged Co-LuxS was expressed in minimal medium plus 100 μM $CoCl_2$ as described above, except that the lysis buffer had no imidazole and the NaCl concentration was 20 mM (instead of 500 mM). The crude lysate was loaded on a Q-Sepharose Fast-Flow column (3 × 8 cm; Amersham Pharmacia Biotech AB) that had been preequilibrated in 25 mM Tris·HCl (pH 7.5) and 20 mM NaCl. The column was washed with 3 column volumes of the above buffer. Elution was carried out with a NaCl gradient (20−500 mM) in the above buffer to yield fractions enriched in Co-LuxS (containing ∼260 mM NaCl). These fractions were pooled (∼35 mL), adjusted to 1 M NaCl, and loaded onto a phenyl-Sepharose fast-flow column (3 × 9 cm; Amersham Pharmacia Biotech AB) at a flow rate of ∼2 mL/min. After the column was washed with 100 mL of a buffer containing 25 mM Tris·HCl (pH 8.0) and 1 M NaCl, the bound LuxS was eluted with the above buffer plus a reverse gradient of 1000−20 mM NaCl (360 mL in 60 min). Metal analyses were performed by inductively coupled plasma emission spectrometry (ICP-ES) at the Chemical Analysis Laboratory of the University of Georgia. Protein concentration was determined by the Bradford method using bovine serum albumin (Sigma) as standard and was corrected by a factor of 0.40 (based on the metal contents of multiple Co-LuxS-HT samples and the assumption that each polypeptide binds one metal ion). When stored in the frozen form at −80 °C, the LuxS proteins were stable for at least 6 months.

Cloning and Purification of Pfs. The gene coding for *B. subtilis* SAH nucleosidase (*12*) was cloned by PCR with genomic DNA as template and primers 5′-GGAAGGCCATATGAGACTAGCAGTCATCGGAGC-3′ and 5′-GAAGCTCGAGATGAATTCGTTTGATCACCTTTAACAC-3′. The PCR product was digested with restriction endonucleases *Nde*I and *Xho*I and subcloned into prokaryotic expression vector pET22b(+). This cloning procedure results in the addition of a six-histidine tag to the C-terminus of the nucleosidase. The identity of the DNA construct was

confirmed by DNA sequencing. Protein expression and purification on a Co(II) affinity column were performed in a manner similar to that described for LuxS.

Assay for LuxS Activity. SRH was prepared by incubating SAH (typically 10 mM) with nucleosidase Pfs (2 μM) for 1 h at room temperature, and the completion of the reaction was monitored spectrophotometrically using the absorption difference between SAH and adenine ($\Delta\epsilon_{276} = -1.4$ mM^{-1} cm^{-1}) (*13*). A typical LuxS reaction (total volume = 1.0 mL) contained 50 mM HEPES (pH 7.0), 150 mM NaCl, 0−68 μM SRH, and 150 μM 5,5′-dithiobis(2-nitrobenzoic acid) (DTNB). The reaction was initiated by the addition of LuxS (final concentration 0.4 μM) and monitored continuously at 412 nm ($\epsilon = 14000$ M^{-1} cm^{-1}) in a Perkin-Elmer λ20 UV−vis spectrophotometer at room temperature.

Inactivation Kinetics of LuxS. Zn(II)-, Co(II)-, or Fe(II)-substituted LuxS-HT and native LuxS (crude) were diluted in the LuxS assay buffer [50 mM HEPES (pH 7.0) and 150 mM NaCl] to a concentration of ~2 mg/mL. The resulting solution was incubated under ambient conditions (23 °C and exposed to air). At various time points (0−10 h), aliquots were withdrawn, and the remaining LuxS activity was determined as described above. LuxS inactivation in the presence of 10 μM H_2O_2 was similarly carried out, except that incubation was performed in an ice−water bath.

Correlation between Fe(II) Content and LuxS Activity. Freshly thawed Fe(II)-LuxS-HT (2.7 mg/mL) was incubated at room temperature, with exposure to atmospheric oxygen. At various times (0−12 h), 10 μL aliquots were withdrawn, and the remaining activity and Fe content were determined (*14*). To measure the Fe(II) content, the protein was denatured by the addition of an equal volume of 8 M guanidine hydrochloride, and 1,10-phenanthroline in 0.5 M sodium acetate (pH 5.0) was added to a final concentration of 8 mM. The absorbance (at 510 nm) of the resulting solution was determined on a UV−vis spectrophotometer. The concentration of Fe(II) was then calculated according to a standard line generated with known concentrations of $Fe(NH_4)_2(SO_4)_2$. To measure the Fe(III) content, the protein was denatured in 1 M HCl and centrifuged at 14000 rpm for 4 min in a microcentrifuge. KSCN was added to the clear supernatant to a final concentration of 0.8 M. The absorbance at 480 nm was determined, and the concentration of Fe(III) was calculated by comparison with the $Fe(NO_3)_3$ standard line.

Mass Spectrometric Analysis of Inactivated LuxS. Zn(II)-, Co(II)-, and Fe(II)-substituted LuxS-HT and LuxS-HT from LB medium were dialyzed in a buffer containing 30 mM Tris·HCl (pH 7.4) and 50 mM ammonium acetate at 4 °C for 24 h and further incubated at 4 °C for >24 h. Each sample was desalted by passing through a ZipTip C-18 column (Millipore), eluted with 50% acetonitrile in water. After the addition of 0.1% trifluoroacetic acid (final concentration), the sample was analyzed on a Micromass Q-TOF II electrospray ionization mass spectrometer.

Absorption Spectroscopy. Concentrated Co(II)-LuxS-HT was diluted in a buffer containing 500 mM sodium phosphate (pH 7.0) and 100 mM NaCl to give a final concentration of 70−80 μM and transferred into a 100 μL quartz microcuvette. SRH was then added to a final concentration of 150−180 μM, and the absorption spectra were recorded on a Hewlett-Packard Model 8452A diode array UV−vis spectrophotometer at 25 °C once every minute.

Preparation of the Deuterated Quinoxaline Derivative. Recombinant Co(II)-LuxS-HT was exchanged into a D_2O buffer (50 mM NaH_2PO_4−Na_2HPO_4, pD 7.0, 50 mM NaCl) in an Amicon concentrator (Millipore). SRH (final concentration 1 mM), Co(II)-LuxS-HT (final concentration 0.8 mg/mL), and 1,2-phenylenediamine (final concentration 2 mM) were mixed in the D_2O buffer (total reaction volume = 1 mL) and incubated at room temperature for 18 h. At this point, the pD of the reaction mixture was adjusted to 4.5 by the addition of deuterated formic acid, and the resulting solution was incubated for an additional 18 h. The reaction mixture was extracted with ethyl acetate (4 × 0.35 mL), and the organic layer was concentrated to dryness under reduced pressure. After being redissolved in methanol (or ethyl acetate), the crude product was purified by reversed-phase HPLC on a semipreparative C-18 column (Vydac). The column was eluted with a 30 min gradient of 10−100% acetonitrile in water (monitored at 240 nm). The desired product eluted at ~40% acetonitrile. ^{1}H NMR (250 MHz, $CDCl_3$): δ 8.09−8.03 (m, 2H, aromatic), 7.73−7.83 (m, 2H, aromatic), 5.16 (dd, 0.6H, C2′-H, $J = 5.5$, 3.5 Hz), 4.08 (dd, 1H, C1′-H, $J = 11.5$, 3.5 Hz), 3.88 (m, 1H, C1′-H), 2.84 (t, 2H, CH_2D, $J = 2.3$ Hz). HRESI-MS (dissolved in H_2O): $C_{11}H_{10}D_2N_2O_2Na^+$ ($[M + Na]^+$) calcd 229.0914, found 228.0849, 229.0900, 230.0967.

Control Reaction 1. This reaction was carried out in exactly the same fashion as described above except that H_2O buffers were used in all steps. ^{1}H NMR (250 MHz, $CDCl_3$): δ 8.17−8.11 (m, 2H, aromatic), 7.88−7.83 (m, 2H, aromatic), 5.21 (dd, 1H, C2′-H, $J = 5.2$, 3.5 Hz), 4.13 (dd, 1H, C1′-H, $J = 11.8$, 3.5 Hz), 3.96 (dd, 1H, C1′-H, $J = 11.8$, 5.2 Hz), 2.91 (s, 3H, CH_3). HRESI-MS (dissolved in H_2O): $C_{11}H_{12}N_2O_2Na^+$ ($[M + Na]^+$) calcd 227.0791, found 227.0804.

Control Reaction 2. This reaction was performed by mixing SRH (1 mM) and Co(II)-LuxS-HT (0.8 mg/mL) in H_2O buffer. After incubation for 18 h, EDTA was added to the reaction (12 mM final concentration), and the solution was heated at 90 °C for 10 min to inactivate the LuxS enzyme. The resulting mixture was cooled and lyophilized to dryness. The residue was redissolved in D_2O (pD adjusted to 4.5) containing 2 mM 1,2-phenylenediamine and let stand at room temperature for 30 h. The quinoxaline product was isolated and analyzed as described above. HRESI-MS (dissolved in H_2O): $C_{11}H_{12}N_2O_2Na^+$ ($[M + Na]^+$) calcd 227.0791, found 227.0800.

Control Reaction 3. This reaction was carried out in the same manner as the positive reaction in D_2O, except that no LuxS was added. The reaction mixture, after incubation for 18 h at room temperature, was directly analyzed by ESI mass spectrometry. No deuterium incorporation into SRH was observed. HRESI-MS (dissolved in D_2O): $C_9H_{11}D_6NO_6SNa^+$ ($[M + Na]^+$) calcd 296.1033, found 296.1015.

RESULTS

Purification of LuxS. As noted previously (*4*, *11*), native LuxS is unstable, undergoing rapid inactivation under ambient conditions (vide infra). This made it difficult to purify the native enzyme from wild-type bacteria. We were only able to partially purify the native *B. subtilis* LuxS by

Table 1: Metal Content and Catalytic Activity of Various LuxS Variants

enzyme	metal content (mol)			k_{cat} (s^{-1})	K_M (μM)	k_{cat}/K_M (M^{-1} s^{-1})
	Fe	Co	Zn			
native	ND[a]	ND	ND	ND	2.5 ± 0.2	ND
LuxS-HT (LB)	0.45	0.15	0.33	0.022 ± 0.003	7.5 ± 0.2	0.29×10^4
Fe-LuxS-HT	0.83	0.08	0.05	0.018 ± 0.003	1.9 ± 0.2	0.90×10^4
Co-LuxS-HT	0.00	0.95	0.05	0.035 ± 0.003	2.3 ± 0.5	1.6×10^4
Zn-LuxS-HT	0.00	0.03	0.83	0.065 ± 0.008	58 ± 7	0.11×10^4
Co-LuxS	0.00	0.95	0.05	0.034 ± 0.001	2.6 ± 0.1	1.3×10^4

[a] ND, not determined.

quickly passing the crude cell lysate through an anion-exchange column (Q-Sepharose). This procedure removed all of the small-molecular-weight thiols that might otherwise interfere with the LuxS activity assay. To obtain the protein in sufficient quantity and purity for mechanistic investigations, we overexpressed the *B. subtilis* enzyme in *E. coli* and purified it to apparent homogeneity. A C-terminally six-histidine-tagged variant (LuxS-HT) was also constructed to facilitate its purification by metal affinity chromatography. This is critical because the native enzyme is unstable. The affinity chromatography allowed us to purify the protein very quickly and to remove any wild-type *E. coli* LuxS from the LuxS mutants.

LuxS is a metalloenzyme, and the metal ion has been proposed as Zn^{2+} (*8*−*10*). It has been noted that the ligand environment of the metal ion has striking similarity to that of peptide deformylase (two histidines, a cysteine, and a water), which contains an Fe^{2+} ion in its native state (*15*, *16*). Further, both peptide deformylase (*17*) and LuxS (*9*, *10*) undergo inactivation under aerobic conditions and form a cysteic acid in the active site. These similarities led us to speculate that the native metal in LuxS might also be Fe^{2+}. To test this notion, we prepared LuxS proteins that are enriched in either Fe, Co, or Zn by adding the corresponding metals into the growth medium. In the case of Co(II)-substituted enzyme, the metal ion would also provide a useful spectroscopic probe for studying its function in the enzyme. The proteins were purified to apparent homogeneity on a cobalt affinity column. Metal analyses show that each of the proteins contained the desired metal ion as the predominant cofactor, whereas the recombinant LuxS-HT derived from Luria−Bertani broth (no added metal) contained 0.45, 0.33, and 0.15 mol of Fe, Zn, and Co per polypeptide, respectively (Table 1). We believe that the small amounts of Co present in Fe-LuxS-HT, Zn-LuxS-HT, and LuxS-HT from LB medium were introduced during purification on the cobalt affinity column. Due to the impure nature of the native LuxS preparation, no metal analysis was conducted for the sample.

Catalytic Properties of LuxS. LuxS activity was determined by measuring the amount of free thiol released (i.e., homocysteine) using Ellman's reagent (*18*). The native LuxS (partially purified) exhibited saturation kinetics toward SRH, with a K_M value of 2.5 μM and V_{max} value of 3.0×10^{-4} μmol mg^{-1} min^{-1} (Figure 2 and Table 1). Fe- and Co-LuxS-HT have similar activities, with K_M values of ~2 μM, k_{cat} values of 0.018−0.035 s^{-1}, and k_{cat}/K_M values of (0.9−1.6) $\times 10^4$ M^{-1} s^{-1}. Zn-LuxS-HT has a 10-fold lower activity ($k_{cat}/K_M = 1120$ M^{-1} s^{-1}), due to a much higher K_M value (58 μM). The LuxS purified from LB medium exhibited an intermediate apparent K_M value (7.5 μM), consistent with the heterogeneous nature of the metal cofactor in the sample.

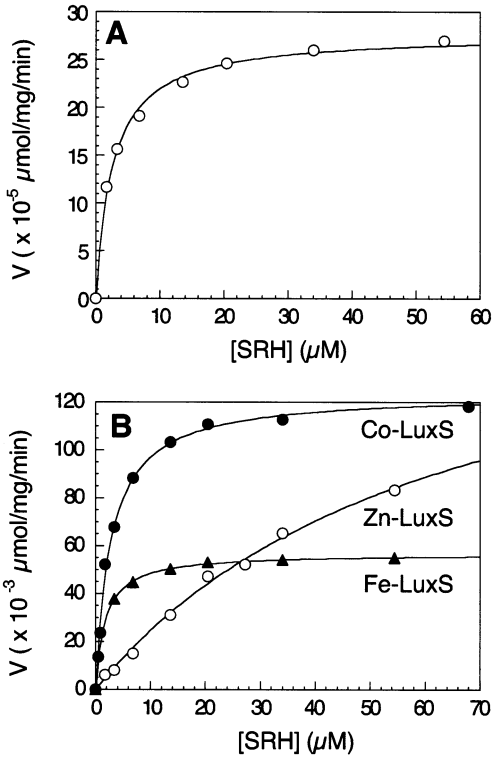

FIGURE 2: Comparison of the catalytic properties of native LuxS (A) with that of various metal-substituted LuxS-HT forms (B). The lines were fitted to the data according to equation $V = V_{max}[S]/(K_M + [S])$.

To determine whether the addition of a C-terminal histidine tag affects the catalytic activity of LuxS, we also prepared Co(II)-substituted wild-type LuxS (no histidine tag) and found that it had the same activity as Co-LuxS-HT (Table 1). The large disparity in the K_M value between the native enzyme and Zn-LuxS-HT suggests that Zn is highly unlikely the metal cofactor in the native enzyme. Instead, the above data are consistent with Fe or Co being the native metal cofactor. Note that the catalytic activity of LuxS (k_{cat}/K_M value) is comparable to that of acylhomoserine lactone synthase, the enzyme responsible for the synthesis of AI-1's (*19*). It has been suggested that, in vivo, AI-2 production is limited by the amount of SAH produced in SAM-dependent methyltransferase reactions (*20*). Thus, there seems to be little evolutionary pressure for further improving the catalytic efficiency of LuxS.

Stability of LuxS Variants. It was reported that native LuxS was extremely labile under aerobic conditions, especially at low concentrations (*4*, *11*). Others have also reported difficulty in obtaining recombinant LuxS of significant catalytic activity (*10*). We examined the stability of various LuxS forms by incubating them under ambient conditions

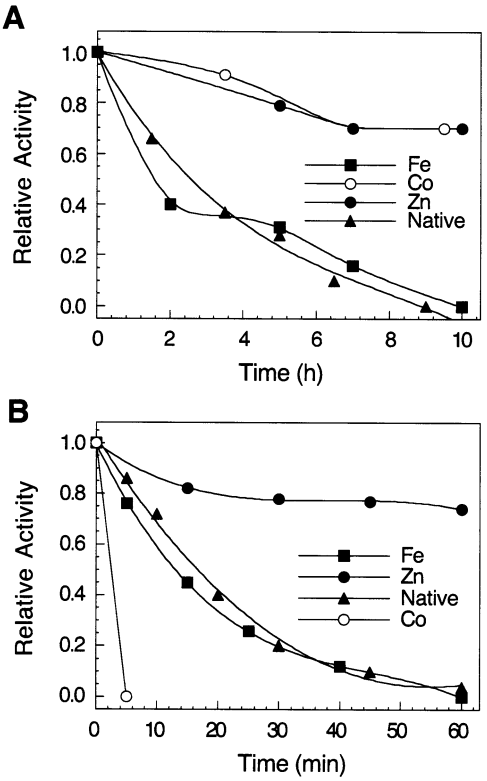

FIGURE 3: Time courses of enzyme inactivation for native LuxS and various metal-substituted LuxS forms under the ambient condition (A) and in the presence of 10 μM H_2O_2 (B). All of the activities are relative to those at time 0.

(23 °C and with exposure to air) for varying lengths of time and measuring the amount of activity that remained. The native and Fe-substituted LuxS both underwent rapid inactivation; further, the two enzymes have very similar inactivation kinetics (both have half-lives of ~2 h) (Figure 3a). In contrast, the Zn- and Co-substituted enzymes were much more stable, retaining ~80% activity after 10 h of incubation. Next, we subjected the enzymes to treatment with 10 μM H_2O_2, which should oxidize Fe(II) into Fe(III). Again, the native enzyme and Fe-LuxS-HT had similar inactivation profiles (half-life ~15 min), whereas Zn-LuxS-HT was essentially unaffected by H_2O_2 (Figure 3b). Surprisingly, Co-LuxS-HT was instantaneously inactivated and precipitated out of solution by H_2O_2, possibly due to oxidation of Co(II) into kinetically inert Co(III). Thus, the stability profile rules out Zn or Co, and is highly suggestive of Fe^{2+}, as the metal ion in the native LuxS enzyme. To ascertain that Fe^{2+}, instead of Fe^{3+}, is the cofactor responsible for the observed LuxS activity, we repeated the above experiment with the recombinant Fe-LuxS-HT and measured the remaining activity as well as the Fe^{2+} and Fe^{3+} contents in the sample at various time points. An excellent correlation between LuxS activity and the Fe^{2+} content was observed, whereas the LuxS activity was inversely correlated with the Fe^{3+} content (Figure 4).

To gain further insight into the mechanism of LuxS inactivation, we analyzed the various LuxS forms that had been incubated overnight under ambient conditions and subsequently acid denatured by ESI mass spectrometry. Both Zn- and Co-LuxS-HT showed a single major peak of 18645 Da in the deconvoluted spectra, consistent with the unmodified protein (Figure 5). The Fe-LuxS-HT and LuxS-HT prepared from LB medium, however, showed a second peak

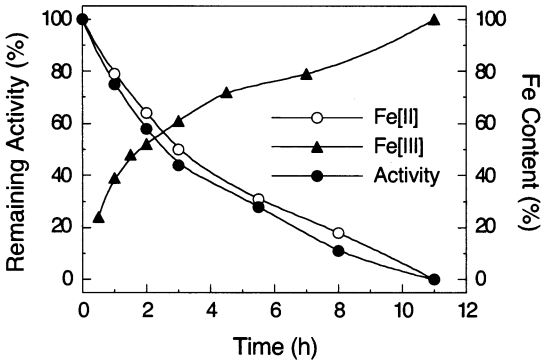

FIGURE 4: Correlation between LuxS activity and Fe(II) content. Fe-LuxS-HT (2.7 mg/mL) was incubated under room temperature with exposure to air, and the remaining activity was measured at the indicated times. LuxS activity and Fe(II) content are relative to the values at time 0, whereas Fe(III) content is relative to that at 11 h.

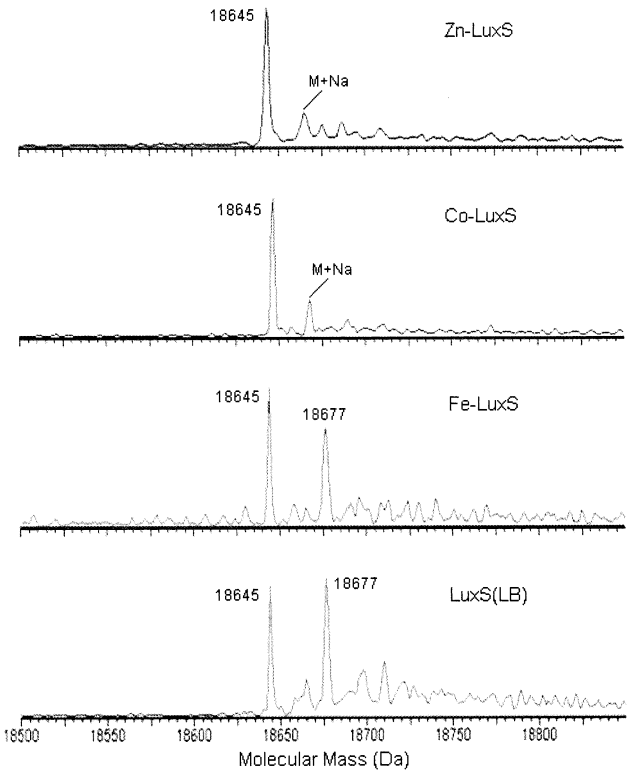

FIGURE 5: ESI-MS analysis of various metal-substituted LuxS-HT forms that had been incubated for >24 h at 4 °C. The spectra shown are the deconvoluted spectra showing the molecular masses of the proteins.

at 18677 Da, in addition to the expected peak at 18645 Da. The increase of ~32 Da in the molecular mass is consistent with the oxidation of a cysteine into cysteinesulfinic acid. Digestion of the inactivated Fe-LuxS-HT by chymotrypsin followed by ESI-MS analysis revealed a peak at *m*/*z* 1015.95 (data not shown). The isotope pattern of the peak indicated that the species was a triply charged ion, derived from a peptide of molecular mass of 3044.8 Da. This mass does not correspond to any chymotryptic fragment of the native protein but is consistent with a LuxS peptide containing a cysteic acid, T^{63}IRSHAEKYDHFDIIDISPMG(Cys-SO_3H)-QTGY^{88} (*12*). Unambiguous sequencing of this peptide by tandem MS was not successful; however, many of the peaks observed were consistent with fragments derived from the

above peptide. These results suggest that, as LuxS was inactivated, Cys-84 underwent oxidation to cysteinesulfinic acid, which was further oxidized to cysteic acid during or after chymotrypsin digestion. A cysteic acid at position 84 was previously observed in the crystal structure of LuxS (*9*, *10*). This is reminiscent of the Fe^{2+} form of peptide deformylase, which also undergoes partial oxidation of an active site cysteine to cysteic acid during its oxygen-mediated inactivation (*17*).

Catalytic Properties of E57 and C84 Mutants. Sequence alignment shows that Glu-57 and Cys-84 are highly conserved residues among LuxS proteins from a diverse set of bacterial organisms (*8*). Both residues are located in the active site of LuxS (*8*−*10*). To determine whether or how they are involved in catalysis, Glu-57 was mutated into Asp, Ala, and Gln, whereas Cys-84 was changed to Ala, Ser, and Asp. All of the mutants were well expressed in the presence of 100 μM Co^{2+} and gave soluble proteins that were purified to apparent homogeneity by metal affinity chromatography. The E57D mutation reduced the activity by 220-fold (K_M = 180 ± 30 μM; k_{cat} = 0.013 ± 0.001 s^{-1}; k_{cat}/K_M = 72 M^{-1} s^{-1}). The E57A and E57Q mutants had no detectable activity (estimated to be $>10^4$-fold reduction) by either Ellman's reagent or derivatization of any DHPD formed with 1,2-phenylenediamine followed by HPLC analysis. This indicates that Glu-57 is essential for catalysis, probably acting as a general acid/base (see Discussion). Both C84S and C84D mutants had drastically reduced activity (>220-fold), which could not be reliably determined by Ellman's reagent, due to background reaction between DTNB and surface cysteine residues in LuxS. However, the presence of residual catalytic activity in these mutants could be unambiguously (albeit qualitatively) demonstrated by the 1,2-phenylenediamine/HPLC assay. On the other hand, the C84A mutant showed no catalytic activity by either assay method. We propose that Cys-84 acts as the second general acid/base during catalysis. Given the structural similarity between aspartic acid and cysteinesulfinic acid, the results suggest that oxidation of Cys-84 should result in inactivation of LuxS.

Involvement of the Metal Ion in Catalysis. The ligand environment of the metal ion (His-54, His-58, Cys-126, and water) suggests that it is a catalytic metal ion. Its involvement in catalysis was assessed by the absorption spectra of Co(II)-substituted LuxS in the absence and presence of substrate SRH. At pH 7.0, the free enzyme displayed three D−D transition bands at 530, 570, and 650 nm (Figure 6a). This spectrum is qualitatively similar to that of peptide deformylase, in which the metal is coordinated by two histidines, a cysteine, and a hydroxide ion (*21*). At pH 10.5, the LuxS spectrum was virtually indistinguishable from that of deformylase (data not shown). This indicates that at pH ≥7, the fourth ligand of LuxS metal is predominantly a hydroxide ion. After addition of SRH, the LuxS spectrum underwent dramatic changes in a time-dependent manner and became featureless (no distinct bands) at 6 min (Figure 6a). Upon further incubation (t = 18 min, when most of the SRH was consumed), however, the spectrum returned to that of the free LuxS form. The same kind of spectral changes were also observed for the E57D mutant, although at a slower rate (data not shown). In contrast, no such changes were observed for the E57A (Figure 6b) or E57Q mutants (data not shown), which are catalytically inactive. The simplest

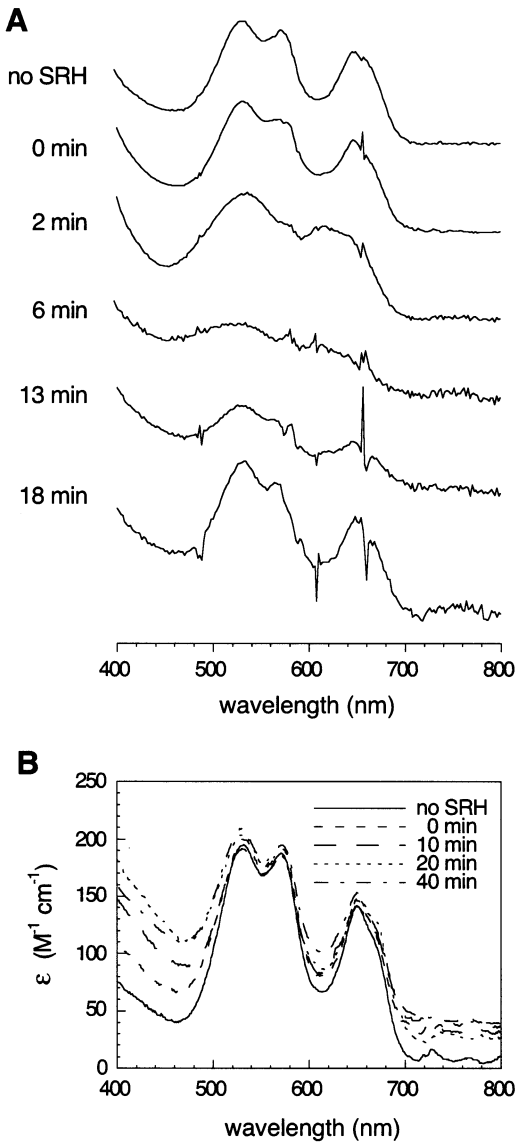

FIGURE 6: Absorption spectra of wild-type (A) and E57A Co-LuxS-HT (B) in the absence and presence of SRH (pH 7.0). Co(II)-LuxS-HT (70−80 μM) was rapidly mixed with SRH (150−180 μM) at time 0, and the absorption spectra were recorded at the specified time points.

interpretation is that the featureless spectrum represents an ensemble of catalytic intermediates, in which the metal ion is coordinated with different keto/enolate ligands.

Deuterium Exchange Experiments. To gain additional mechanistic insight into the LuxS-catalyzed reaction, we performed the enzymatic reaction in D_2O using Co-LuxS-HT and monitored deuterium incorporation into the reaction products by NMR spectroscopy and mass spectrometry. Due to the difficulty in directly isolating DHPD or the furanone derivative by HPLC, we carried out the reaction in the presence of 1,2-phenylenediamine, which reacted in situ with DHPD to form a single, stable quinoxaline derivative (Scheme 1). 1,2-Phenylenediamine had no effect on LuxS activity. The quinoxaline derivative was readily purified by HPLC. While the quinoxaline derivative derived from reactions carried out in H_2O showed a molecular ion at m/z 227.0804 (calculated mass for $C_{11}H_{12}N_2O_2Na$ = 227.0791), its counterpart from the D_2O reaction (after being redissolved in H_2O) showed three peaks at m/z 228.0849 (intensity

Scheme 1

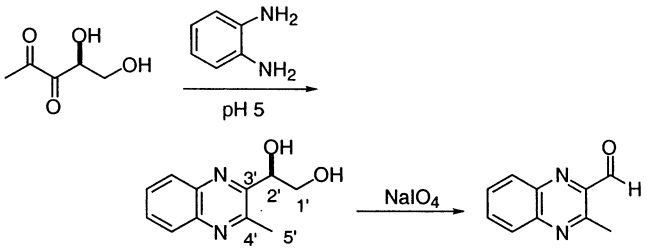

100%), 229.0900 (67%), and 230.0967 (30%). Oxidation of the deuterated quinoxaline derivative with $NaIO_4$ resulted in an aldehyde that showed only two peaks at *m*/*z* 196.0595 and 197.0700 (M + Na). This indicates that one of the deuterium labels was incorporated at the C1′ position and was lost upon oxidative cleavage of the 1,2-diol (Scheme 1). In the ^{1}H NMR spectrum, the unlabeled compound had a sharp singlet at δ 2.9 for the C5′ methyl group and three double doublets in the δ 3.9−5.2 region for the C1′ and C2′ protons (Figure 7a). The quinoxaline derivative from the D_2O reaction showed several different features (Figure 7b). First, the methyl group signal became a broadened triplet of only two protons (the aromatic protons were used as internal standards). Second, the C2′ proton signal (δ 5.2) was decreased to ∼0.6 H, consistent with ∼40% deuterium incorporation at this position. Finally, the signals of the C1′ protons became more complex but are consistent with the overlap of a broadened doublet (from 40% C2′ deuterated species) on top of a double doublet (from 60% C2′ nondeuterated species). Thus, the NMR and MS data show that one of the C5′ methyl protons, ∼40% of the C2′ proton, and ∼10% of a C1′ proton were replaced by deuterium. In contrast, no deuterium was detected in the product if the LuxS reaction was first carried out in H_2O and the DHPD obtained was then reacted with 1,2-phenylenediamine in D_2O. No deuterium was incorporated into the substrate when SRH was incubated in D_2O in the absence of LuxS. Broadening and splitting of the methyl signal are caused by the coupling interaction between the two remaining protons and the deuterium (J = 2.3 Hz).

DISCUSSION

LuxS activity was observed in the crude cell lysate more than 3 decades ago (*4*, *11*). It was thought to be part of the catabolic pathway for detoxifying SAH, a potent inhibitor of many methyltransferases that utilize SAM as the cofactor. More recent studies revealed an important second function of LuxS, i.e., the biosynthesis of AI-2 (*6*). Since quorum-sensing regulates the expression of many bacterial genes including those for bacterial virulence, the enzymes involved in quorum sensing are being considered as targets for designing novel antibiotics (*22*, *23*). There have been several reports on the mechanistic investigation of the nucleosidase Pfs (*22*, *24*−*26*), but none on LuxS, apparently due to its instability and thus difficulty in its purification and characterization. In this work, we have shown that LuxS is an iron enzyme, and the Co(II)-substituted LuxS has wild-type activity and is much more stable. In addition, the electronic properties of the Co(II) ion are highly dependent upon the identity and symmetry of its ligand environment, providing a sensitive spectroscopic probe for studying the structure−function relationship in this enzyme.

Identity of the Metal Ion. Ideally, one should purify the native enzyme from the wild-type (nonoverproducing) bacterium and conduct metal analysis to establish the metal identity. This has not been possible for LuxS, however, due to instability of the native enzyme (*4*, *11*). By generating a recombinant, C-terminally histidine-tagged variant, we were able to rapidly purify LuxS containing various metal cofactors including Fe^{2+} by metal affinity chromatography. When the recombinant *E. coli* cells were grown in LB medium (without additional metal ions), the purified LuxS contained 45% Fe, 33% Zn, and 15% Co (Table 1). None of the other common metal ions (other metals tested include Al, B, Ba, Ca, Cd, Cr, Cu, Mg, Mn, Mo, Ni, Pb, and Sr) were present in the samples at significant levels. Given the fact that Fe and Zn are among the most abundant metals in nature, the above result suggests that the metal ion in native LuxS should be Fe, Zn, or Co. Indeed, LuxS proteins containing Fe, Zn, or Co can be prepared by simply adding the respective metals into the growth medium and are all catalytically competent. To determine which metal is the native cofactor, we

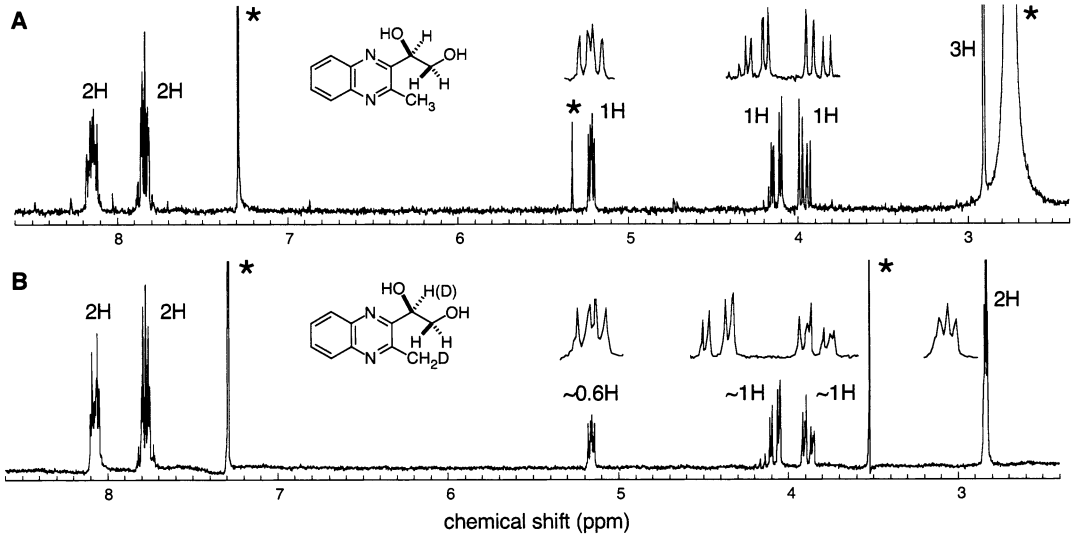

FIGURE 7: NMR spectra (250 MHz, $CDCl_3$) of the quinoxaline derivatives derived from H_2O (A) and D_2O reactions (B). The peaks labeled with asterisks are derived from solvents and unknown contaminants.

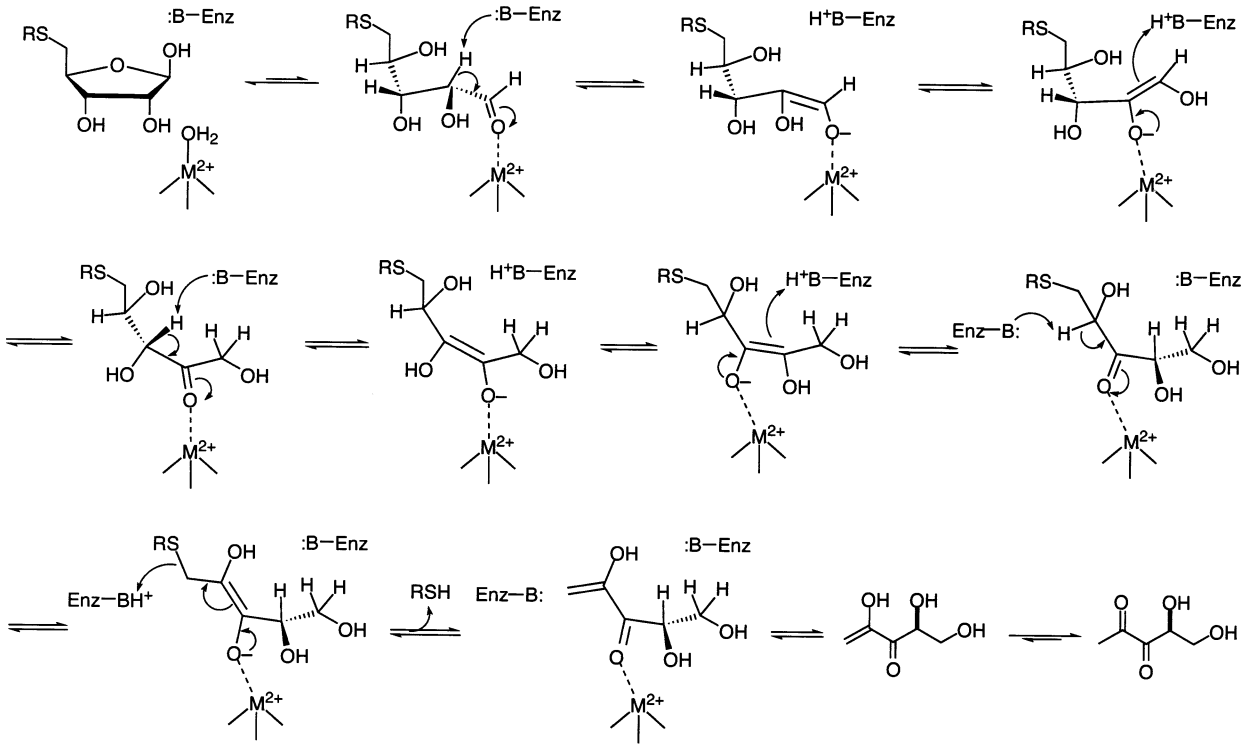

FIGURE 8: Proposed mechanism for LuxS-catalyzed reaction.

compared the properties of the recombinant proteins with those of native LuxS. We found that the Fe-LuxS-HT shares all of the traits of the native enzyme. For example, they both have the same K_M value toward SRH (~2 μM); they undergo time-dependent inactivation under aerobic conditions as well as when treated with H_2O_2 (Figure 3). On the other hand, Zn-LuxS-HT has a much higher K_M value (58 μM) and is very stable under aerobic conditions or in the presence of H_2O_2. While the Co-LuxS-HT has catalytic properties similar to those of the native enzyme, it is stable under aerobic conditions. It did undergo inactivation upon treatment with H_2O_2, but with drastically different kinetics. On the basis of these results and its remarkable similarity to the Fe^{2+} center in peptide deformylase, we conclude that the native enzyme contains an Fe^{2+} ion. The small amount of Co in the LuxS sample (from LB medium) is most likely due to metal exchange during affinity chromatography on the cobalt(II) column. The 33% Zn content is probably an artifact of overexpression. The large amounts of polypeptides synthesized presumably depleted the Fe supply in the cell; the additional polypeptides picked up any metal ions that were both available and functional (in terms of fitting in the metal-binding site). This phenomenon has previously been observed for a number of other Fe-containing proteins including peptide deformylase (*27*−*29*).

Mechanism of LuxS Inactivation. Our results show that the inactivated LuxS contained an oxidized cysteine at position 84, which is a highly conserved residue in the active site. However, oxidation of Cys-84 is most likely a consequence rather than the cause of LuxS inactivation, as an Fe-LuxS-HT sample that had been completely inactivated showed only partial oxidation at Cys-84 (~40%) (Figure 5). This is reminiscent of peptide deformylase, which also undergoes partial oxidation of an active site cysteine (*17*). Also like the deformylase, LuxS inactivation is uniquely associated with the Fe enzyme form; no cysteine oxidation was observed for either Zn- or Co-LuxS. We propose an inactivation mechanism similar to that of peptide deformylase, in which molecular oxygen binds to the Fe^{2+} center by displacing the water/hydroxide ligand and oxidizes it to Fe^{3+}, leading to enzyme inactivation (*17*). In the case of deformylase, the superoxide radical anion formed diffuses out of the active site (leaving no protein oxidation) and disproportionates into O_2 and H_2O_2. The peroxide subsequently inactivates a second Fe^{2+} enzyme through a Fenton-like reaction, causing oxidation of the active site cysteine in the second protein molecule. Note that Fe^{2+}-LuxS undergoes rapid inactivation upon treatment with H_2O_2 (Figure 3). Other divalent metal ions such as Zn^{2+} and Co^{2+} are not (or less) susceptible to oxidation by molecular oxygen, and therefore, LuxS substituted with these metal ions is expected to be stable under aerobic conditions, as is observed. Other investigators reported that the recombinant LuxS contained both Zn as the metal cofactor and a cysteic acid at position 84 (*8*−*10*). We believe that their recombinant LuxS initially contained a mixture of Fe^{2+} and Zn^{2+} in the active site. During purification and crystallization, the Fe^{2+} ion was oxidized to Fe^{3+}, causing partial oxidation of Cys-84. Due to the very different ligand preference, the Fe^{3+} ion leaked out of the enzyme, leaving behind a mixture of intact Zn-containing enzyme and the oxidized apoprotein.

Catalytic Mechanism. On the basis of the above observations, we propose the following mechanism for the LuxS-catalyzed reaction (Figure 8). SRH exists as an equilibrium between the free aldehyde and hemiacetal forms. In the E•S complex, the aldehyde carbonyl is coordinated to the metal ion, displacing the bound water/hydroxide in the free enzyme. Coordination to the metal increases the acidity of the C2′ proton, which is abstracted by a general base in the active site. The enolate formed undergoes ligand exchange with

the C2′-OH group, presumably assisted by a second general base/acid and through a five-membered-ring transition state. Tautomerism back to the keto form generates a carbonyl at the C2′ position, with reprotonation at the C1′ position. Repetition of the above sequence shifts the carbonyl group to the C3′ position. The 3′-keto intermediate is similar to that found in the mechanism of SAH hydrolase (*7*). Subsequent β-elimination, probably catalyzed by the second (or a third) general base, results in the release of homocysteine as a free thiol and the formation of DHPD in its enol form. The enol spontaneously tautomerizes to the keto form, either on its way to or after leaving the active site.

The above mechanism is consistent with all of the experimental observations. First, it readily explains the observed deuterium incorporation at C1′, C2′, and C5′ positions. Incomplete exchange at the C1′ and C2′ positions can be explained by the restricted access of the general acid/base residues to solvent molecules. The crystal structure of the LuxS/SRH complex shows that the ribose ring is deeply buried and that two conserved residues, Cys-84 and Glu-57, are properly positioned to act as the first and second general acids/bases, respectively (*10*). Removal of either acid/base functionality (as in E57A and C84A mutants) resulted in total loss of activity. Further, both residues are monoprotic, a feature that favors the retention of substrate-derived protons. The mechanism also suggests that the proton removal/addition at C1′−C3′ is mediated by the same residue (probably Cys-84) and occurs on the same face of the substrate (Figure 8). It thus predicts stereochemical retention at the C2′ position, as was observed experimentally (*3*).

Second, the proposed mechanism can explain the spectroscopic properties of Co-LuxS. The free enzyme has a set of well-defined D−D transition bands, which are consistent with hydroxide/water as the fourth ligand. Immediately after the addition of SRH, there was essentially no change in the spectrum. This may be due to extremely slow substrate binding or no ligand change upon substrate binding. We believe that the latter is the case, since the catalytically inactive mutants (e.g., E57A) showed no spectral change even after prolonged incubation with SRH. Further, the X-ray crystal structure of the LuxS/SRH complex indicates that the bound SRH is in the furanose (hemiacetal) form and is not directly ligated to the metal ion (*10*). That is because the furanose form is energetically more stable than the free aldehyde form. However, according to our mechanism, catalysis can only occur with the aldehyde form and involves the displacement of the metal-bound water/hydroxide by the carbonyl oxygen. As catalysis takes place, the equilibrium is shifted toward the aldehyde, which is subsequently converted into a series of metal-bound keto/enolate intermediates. Thus, the broad, featureless band in the absorption spectrum (Figure 6 at 6 min) can best be explained as the ensemble of all these intermediates as well as any remaining free enzyme. Upon prolonged incubation, the substrate is consumed, and the enzyme returns to the free enzyme form. The inactive mutants lack the ability to shift the equilibrium, and therefore there is no spectral change.

Third, the mechanism offers a plausible explanation for the observed difference in activity between Zn-LuxS-HT (K_M = 58 μM) and Fe- or Co-LuxS-HT (K_M ~2 μM). Zn^{2+} is a stronger Lewis acid than either Fe^{2+} or Co^{2+}, and the Zn^{2+}-bound water has a lower pK_a (*30*). This means that, at neutral pH, a higher percentage of Zn-LuxS-HT is in the metal-bound hydroxide form, which makes it more difficult for the aldehyde carbonyl to displace the Zn^{2+}-bound water/hydroxide and, hence, the higher K_M value for the Zn enzyme. The same argument also explains why all three enzyme forms (Fe, Co, and Zn) have increasing K_M values with pH (unpublished results).

Finally, although the LuxS mechanism is highly unusual, the various steps of this mechanism have been observed in other enzymes. Oxidation of the ribose C3′-hydroxyl into a keto group followed by β-elimination has been observed in SAH hydrolase (*7*). Metal ion-catalyzed enolization of carbonyl compounds also occurs in glyoxalase I (*31*), xylose isomerase (*32*), L-fuculose-1-phosphate aldolase (*33*), and 6-pyruvoyltetrahydropterin synthase (*34*). In the latter case, a cysteine (Cys-42) was proposed as the general base for α-H abstraction, and Glu-133 facilitates the proton transfer from a Zn^{2+}-bound hydroxyl group.

Conclusion. We have shown that the metal cofactor in native LuxS is an Fe^{2+} ion and that its instability is associated with the oxidation of Fe^{2+} by oxygen. Replacement of the native metal with Co^{2+} results in a stable enzyme of wild-type activity. Spectroscopic investigation of the Co-LuxS revealed a catalytic role for the metal ion, presumably as a Lewis acid during catalysis. Site-directed mutagenesis indicates that Glu-57 and Cys-84 are essential for catalysis, most likely as general acids/bases. The catalytic mechanism likely proceeds through an internal redox reaction that shifts the carbonyl double bond from the C1′ position to the C3′ position, followed by β-elimination at the C4′ and C5′ positions.

ACKNOWLEDGMENT

We thank Dr. Kari Green-Church and Ms. Susan Hatcher for assistance in the MS analyses.

REFERENCES

1. Miller, M. B., and Bassler, B. L. (2001) *Annu. Rev. Microbiol. 55*, 165−199.
2. Bassler, B. L., Wright, M., Showalter, R. E., and Silverman, M. R. (1993) *Mol. Microbiol. 9*, 773−786.
3. Chen, X., Schauder, S., Potier, N., Van Dorsselaer, A., Pelczer, I., Bassler, B. L., and Hughson, F. M. (2002) *Nature 415*, 545−549.
4. Miller, C. H., and Duerre, J. A. (1968) *J. Biol. Chem. 243*, 92−97.
5. Surette, M. G., Miller, M. B., and Bassler, B. L. (1999) *Proc. Natl. Acad. Sci. U.S.A. 96*, 1639−1644.
6. Schauder, S., Shokat, K., Surette, M. G., and Bassler, B. L. (2001) *Mol. Microbiol. 41*, 463−476.
7. Palmer, J. L., and Abeles, R. H. (1979) *J. Biol. Chem. 254*, 1217−1225.
8. Lewis, H. A., Furlong, E. B., Laubert, B., Eroshkina, G. A., Batiyenko, Y., Adams, J. M., Bergseid, M. G., Marsh, C. D., Peat, T. S., Sanderson, W. E., Sauder, J. M., and Buchanan, S. G. (2001) *Structure 9*, 527−537.
9. Hilgers, M. T., and Ludwig, M. L. (2001) *Proc. Natl. Acad. Sci. U.S.A. 98*, 11169−11174.
10. Ruzheinikov, S. N., Das, S. K., Sedelnikova, S. E., Hartley, A., Foster, S. J., Horsburgh, M. J., Cox, A. G., McCleod, C. W., Mekhalfia, A., Balckburn, G. M., Rice, D. W., and Baker, P. J. (2001) *J. Mol. Biol. 313*, 111−122.
11. Duerre, J. A., and Miller, C. H. (1966) *J. Bacteriol. 91*, 1210−1217.
12. Kunst, F., Ogasawara, N., Moszer, I., Albertini, A. M., Alloni, G., Azevedo, V., et al. (1997) *Nature 390*, 249−256.

13. Versees, W., Decanniere, K., Pelle, R., Depoorter, J., Brosens, E., Parkin, D. W., and Steyaert, J. (2001) *J. Mol. Biol. 307*, 1363−1379.
14. Vogel, A. I. (1961) *A Textbook of Quantitative Inorganic Analysis Including Elementary Instrumental Analysis*, 3rd ed., pp 785−787, John Wiley and Sons, New York.
15. Giglione, C., Pierre, M., and Meinnel, T. (2000) *Mol. Microbiol. 36*, 1197−1205.
16. Pei, D. (2001) *Emerging Ther. Targets 5*, 23−40.
17. Rajagopalan, P. T. R., and Pei, D. (1998) *J. Biol. Chem. 273*, 22305−22310.
18. Ellman, G. L. (1959) *Arch. Biochem. Biophys. 82*, 70−77.
19. Parsek, M. R., Val, D. L., Hanzelka, B. L., Cronan, J. E., Jr., and Greenberg, E. P. (1999) *Proc. Natl. Acad. Sci. U.S.A. 96*, 4360−4365.
20. Winzer, K., Hardie, K. R., Burgess, N., Doherty, N., Kirke, D., Holden, M. T. G., Linforth, R., Cornell, K. A., Taylor, A. J., Hill, P. J., and Williams, P. (2002) *Microbiology 148*, 909−922.
21. Rajagopalan, P. T. R., Grimme, S., and Pei, D. (2000) *Biochemistry 39*, 779−790.
22. Cornell, K. A., Swarts, W. E., Barry, R. D., and Riscoe, M. K. (1996) *Biochem. Biophys. Res. Commun. 228*, 724−732.
23. Bassler, B. L. (2002) *Cell 109*, 421−424.
24. Ragione, F. D., Porcelli, M., Carteni-Farina, M., and Zappia, V. (1985) *Biochem. J. 232*, 335−341.
25. Gatel, M., Muzard, M., Guillerm, D., and Guillerm, G. (1996) *Eur. J. Med. Chem. 31*, 37−41.
26. Allart, B., Gatel, M., Guillerm, D., and Guillerm, G. (1998) *Eur. J. Biochem. 256*, 155−162.
27. Rajagopalan, P. T. R., Yu, X. C., and Pei, D. (1997) *J. Am. Chem. Soc. 119*, 12418−12419.
28. Eidsness, M. K., O'Dell, S. E., Kurtz, D. M., Robson, R. L., and Scott, R. A. (1992) *Protein Eng. 5*, 367−371.
29. Czaja, C., Litwiller, R., Tomlinson, A. J., Naylor, S., Tavares, P., LeGall, J., Moura, J. J. G., Moura, I., and Rusnak, F. (1995) *J. Biol. Chem. 270*, 20273−20277.
30. Bertini, I., and Luchinat, C. (1994) in *Bioinorganic Chemistry* (Bertini, I., Gray, H. B., Lippard, S. J., and Valentine, J. S., Eds.) pp 37−107, University Science Books, Sausalito, CA.
31. Sellin, S., Eriksson, L. E. G., and Mannervik, B. (1982) *Biochemistry 21*, 4850−4857.
32. Whitlow, M., Howard, A. J., Finzel, B. L., Poulos, T. L., Winbourne, E., and Gilliland, G. I. (1991) *Proteins*: *Struct., Funct., Genet. 9*, 153−173.
33. Dreyer, M. K., and Schulz, G. E. (1996) *J. Mol. Biol. 259*, 458−466.
34. Burgisser, D. M., Thony, B., Redweik, U., Hess, D., Heizmann, C. W., Huber, R., and Nar, H. (1995) *J. Mol. Biol. 253*, 358−369.

BI034289J